Stochastic analysis of bistability in coherent mixed feedback loops combining transcriptional and post-transcriptional regulations

Mor Nitzan,[1,2] Yishai Shimoni,[1,2,3] Oded Rosolio,[1] Hanah Margalit,[2] and Ofer Biham[1]

[1] *Racah Institute of Physics, The Hebrew University, Jerusalem 91904, Israel*

[2] *Department of Microbiology and Molecular Genetics, IMRIC, Faculty of Medicine, The Hebrew University, Jerusalem 91120, Israel*

[3] *Center for Computational Biology and Bioinformatics (C2B2), Columbia University, New York, NY, USA*

arXiv:1412.0986v1 [q-bio.MN] 2 Dec 2014

Abstract

Mixed feedback loops combining transcriptional and post-transcriptional regulations are common in cellular regulatory networks. They consist of two genes, encoding a transcription factor and a small non-coding RNA (sRNA), which mutually regulate each other's expression. We present a theoretical and numerical study of coherent mixed feedback loops of this type, in which both regulations are negative. Under suitable conditions, these feedback loops are expected to exhibit bistability, namely two stable states, one dominated by the transcriptional repressor and the other dominated by the sRNA. We use deterministic methods based on rate equation models, in order to identify the range of parameters in which bistability takes place. However, the deterministic models do not account for the finite lifetimes of the bistable states and the spontaneous, fluctuation-driven transitions between them. Therefore, we use stochastic methods to calculate the average lifetimes of the two states. It is found that these lifetimes strongly depend on rate coefficients such as the transcription rates of the transcriptional repressor and the sRNA. In particular, we show that the fraction of time the system spends in the sRNA dominated state follows a monotonically decreasing sigmoid function of the transcriptional repressor transcription rate. The biological relevance of these results is discussed in the context of such mixed feedback loops in *Escherichia coli*.

I. INTRODUCTION

Recent studies of the interactions between molecules in living cells revealed a complex interplay between regulatory interactions. The regulatory mechanism that was most thoroughly investigated is transcriptional regulation, in which transcription factor (TF) proteins bind to specific promoter sites on the DNA and regulate the transcription of downstream genes. Recently, the significance of post-transcriptional regulation by small non-coding RNA (sRNA) molecules has been recognized, and is now known to play a major role in cellular processes [1–6]. It was suggested that this regulation mechanism would be energetically efficient, since the sRNA molecules are relatively short and are not translated into proteins [5]. More recently, a quantitative analysis has shown that post-transcriptional regulation by sRNAs provides fine tuning of the regulation strength [7] and is advantageous when fast responses to external stimuli are needed [4, 8, 9].

Regulatory interactions (such as the ones presented above) can be described by a network in which genes and their products are represented by nodes, while the interactions between them are represented by edges. Analysis of such networks revealed structural modules or motifs, such as the auto-regulator and the feed-forward loop, which occur significantly more than randomly expected, and are expected to be of functional importance [10–13]. Some of these motifs include only transcriptional regulation, while others combine different layers of regulation [8, 12–15].

An important class of modules is the feedback loop, consisting of two genes, a and b, that regulate each other's expression. A well studied example of such module, in which both regulations are at the transcriptional level, is the λ switch in *E. coli* [16]. Such transcriptional feedback loop, referred to as the genetic toggle switch, was constructed using methods of synthetic biology and was shown to exhibit bistability [17]. Subsequent theoretical and numerical studies established the conditions under which bistability takes place in such systems [18–24].

In mixed feedback loops (MFLs), the two genes regulate each other using two different regulation mechanisms. A common form of MFLs involves a gene a that expresses a TF and regulates gene b via transcriptional regulation, while gene b transcribes a sRNA and regulates gene a via post-transcriptional regulation by sRNA-mRNA interaction. In general, both the transcriptional regulator and the post-transcriptional regulator can act to either inhibit or

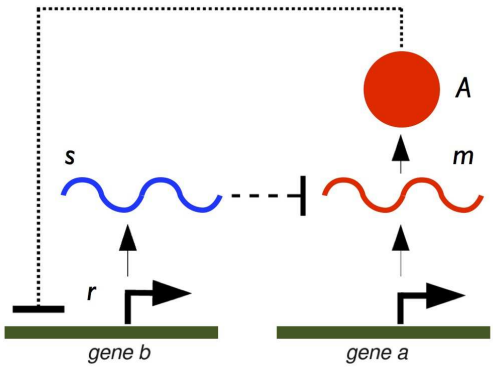

FIG. 1: (Color online) Schematic plot of the mixed feedback loop. Gene a is transcribed into mRNAs (m), which are translated into transcriptional repressor proteins (A). Gene b is transcribed into sRNAs (s), which are not translated into proteins. The A repressors negatively regulate the transcription of gene b by binding to its promoter (the bound repressor is denoted by r). The sRNAs transcribed by gene b bind to the mRNAs of gene a and inhibit their translation. Truncated arrows represent negative regulation.

activate their target. MFLs in which both regulations are negative (double-negative MFLs) belong to the class of coherent feedback loops in which the number of negative regulations is even. The positive-negative MFLs belong to the class of incoherent feedback loops. In general, coherent feedback loops tend to exhibit bistability while incoherent feedback loops tend to exhibit oscillations, under appropriate parameter settings. Schematic representation of the coherent MFL is shown in Fig. 1.

Integration of the transcriptional regulation network and the network of sRNA-mRNA interactions in *E. coli* has revealed that MFLs play important roles in various cellular contexts [8]. A textbook example of such a module is the coherent MFL that consists of the TF Fur and the sRNA RyhB, involved in iron metabolism [25–27]. Another example of a coherent MFL in *E. coli* consists of the TF Lrp and the sRNA MicF, involved in cellular response to variation in nutrient availability [28].

Other examples of MFLs involving noncoding RNAs (microRNAs) were found in the human regulatory network, playing a role in human granulopoiesis [29], various cancers [30] and monocytic differentiation and maturation [31]. Further examples of MFLs were also found in *Drosophila melanogaster* [32], in *Vibrio harveyi* [33], and in *Caenorhabditis elegans* [34]. The identification of feedback loops and mixed-feedback loops in the regulatory

networks of various organisms hints to their important regulatory functions [35].

The dynamic behavior of MFLs involving protein-protein interaction was analyzed theoretically using deterministic analysis in the framework of rate equation models [36]. It was shown that within suitable ranges of parameters, the double-negative (coherent) MFL exhibits bistability, while the positive-negative (incoherent) MFL exhibits oscillations. Similar results were recently obtained for MFLs involving sRNAs [37] and microRNAs [38].

Gene regulation processes are affected by fluctuations due to the stochastic nature of biochemical reactions and the fact that some of the molecules involved appear in low copy numbers. Therefore, in order to obtain a more complete understanding of the dynamic behavior of coherent MFLs and the emergence of bistability it is important to analyze these systems using stochastic methods which take into account the discrete nature of the interacting RNAs and proteins as well as the effects of fluctuations. Fluctuations in MFLs were previously characterized using stochastic methods [39, 40]. However, the lifetimes of the two bistable states and their dependence on the model parameters have not been studied.

In this paper we present a comprehensive analysis of the dynamics of a mixed coherent MFL involving transcriptional regulation and sRNA-mRNA interaction. The analysis is done using a combination of deterministic and stochastic methods, enabling us to identify the stable states of this system as well as the spontaneous, fluctuation-driven transitions between them. We calculate the average lifetimes of the two bistable states vs. parameters such as the transcription rates. As expected, we show that as the transcription rate of the mRNA, g_m, is increased, the average lifetime of the state dominated by the transcriptional repressor, τ_a, increases, while the average lifetime of the state dominated by the sRNA, τ_s, decreases. Thus, for small values of g_m the system spends most of its time in the sRNA dominated state, while for large values of g_m it spends most of the time in the state dominated by the transcriptional repressor. This means that in the two limits the domination times of the two regulators are biased towards one of the two bistable states. The biological relevance of these observations is discussed in the context of such MFLs apparent in *E. coli*.

The paper is organized as follows. In Sec. II we present a deterministic analysis of the MFL and the results for the range of parameters in which bistability appears. In Sec. III we present a stochastic analysis, calculating the average lifetimes of the two bistable states vs. suitable parameters. The results are summarized and their biological relevance is discussed in Sec. IV. In Appendix A we present a detailed account of the experimental data we have

used and the considerations we have made in order to determine the biologically relevant values of the rate coefficients used in our model. In Appendix B we extend the analysis of the bifurcation diagrams to a broader family of parameter variations and to the case in which the transcriptional repressor exhibits cooperative binding.

II. DETERMINISTIC ANALYSIS

Consider an MFL in which gene a encodes a transcription factor and gene b encodes a small RNA. Gene a negatively regulates gene b by transcriptional regulation, while gene b negatively regulates gene a post-transcriptionally via sRNA-mRNA interaction. In this system gene a is transcribed into mRNA molecules, denoted by m, which are translated into transcriptional repressor proteins, denoted by A. Gene b is transcribed into sRNA molecules, denoted by s. The transcriptional repressors A negatively regulate gene b by binding to its promoter site, while the sRNAs negatively regulate gene a by binding to mRNA molecules, destabilizing them and inhibiting their translation.

Here we describe the dynamics of a single MFL, namely one TF gene and one sRNA gene, using rate equations. We denote the levels or copy numbers of the sRNA and mRNA molecules in the cell by s and m, respectively. The level of the sRNA-mRNA complex is denoted by C. The number of free A proteins is denoted by A. The number of A proteins that are bound to the promoter site of gene b is denoted by r. For simplicity, we consider the case in which the regulation is performed by a single copy of the bound repressor. In this case, r takes values in the range $0 \leq r \leq 1$.

The rate coefficients g_m and g_s denote the transcription rates of genes a and b, respectively. The translation rate of gene a, namely the generation rate of A proteins per copy of the mRNA molecule is denoted by g_A. The degradation rates of the sRNAs, mRNAs and the A proteins are denoted by d_s, d_m and d_A, respectively. The binding rate of A proteins to the promoter site of gene b is denoted by c_g and their dissociation rate from the promoter is denoted by u_g. The binding rate of sRNA and mRNA molecules to form a complex is denoted by c_{ms}. The sRNA-mRNA complex degrades at rate d_c, or dissociates into its sRNA and mRNA components at rate u_c. The processes taking place in the MFL and their rates are listed in Table I.

TABLE I : The processes and respective rates in the MFL module.

	Process	**Rate**
1	$\emptyset \rightarrow m$	g_m
2	$m \rightarrow \emptyset$	$d_m m$
3	$m + s \rightarrow C$	$c_{ms} ms$
4	$C \rightarrow m + s$	$u_c C$
5	$\emptyset \rightarrow s$	$g_s(1 - r)$
6	$s \rightarrow \emptyset$	$d_s s$
7	$m \rightarrow m + A$	$g_A m$
8	$A \rightarrow \emptyset$	$d_A A$
9	$A \rightarrow r$	$c_g A(1 - r)$
10	$r \rightarrow A$	$u_g r$
11	$C \rightarrow \emptyset$	$d_c C$

In Appendix A we consider the biologically relevant range of values of each of the rate coefficients used in the analysis of the MFL. These values are determined on the basis of experimental results and related considerations and interpretation. For the calculations and simulations presented below we chose a default value for each parameter, within the biologically relevant range. These default parameter values, g_m=0.007, g_s=0.43, g_A=0.05, d_m=0.003, d_s=0.0008, d_A=0.001, c_{ms}=0.02, c_g=0.08 and u_g=0.01, are used in all the Figures presented in this paper (unless stated otherwise). All the parameters are in units of $\sec^{-1}$.

The rate equations that describe this system take the form

$$\frac{dm}{dt} = g_m - d_m m - c_{ms} m \cdot s + u_c C \tag{1a}$$

$$\frac{ds}{dt} = g_s(1 - r) - d_s s - c_{ms} m \cdot s + u_c C \tag{1b}$$

$$\frac{dA}{dt} = g_A m - d_A A - c_g A(1 - r) + u_g r \tag{1c}$$

$$\frac{dr}{dt} = c_g A(1 - r) - u_g r \tag{1d}$$

$$\frac{dC}{dt} = c_{ms} m \cdot s - d_c C - u_c C, \tag{1e}$$

where Eqs. (1a) and (1b) account for the time dependent levels of the mRNAs and sRNAs, respectively. Each of these equations includes a transcription term and a degradation term. They also include binding terms, which describe the formation rate of the sRNA-mRNA complex, and a term which represents the dissociation of the complex. The transcription term of s includes the factor $1-r$, which accounts for the fact that transcription takes place only when there is no A repressor bound to the b promoter. Eq. (1c) accounts for the time dependent level of the A protein, and includes translation and degradation terms as well as terms describing the binding/unbinding to/from the b promoter. Eq. (1d) accounts for the level of A proteins which are bound to the b promoter. Eq. (1e) accounts for the level of the sRNA-mRNA complex.

The rate equations can be solved by direct numerical integration. For fixed values of the parameters and for a given choice of the initial conditions, the system tends to converge to a steady state. Coherent feedback loops such as the MFL tend to exhibit bistabily within a suitable range of parameters. In such cases, the steady state to which the rate equations converge depends on the initial conditions. Within the rate equation model, once the system converges to one of the bistable states, it remains there and does not switch to the other state.

Under steady state conditions (or in the limit in which the formation and dissociation processes of the sRNA-mRNA complex are fast) the effect of the dissociation process on the RNA and protein levels can be accounted for by a suitable adjustment of the binding rate coefficient c_{ms}. Therefore, the dissociation process is expected to be of secondary importance and does not affect the essential properties of the MFL.

In the analysis presented below it is assumed, for simplicity, that the dissociation rate $u_c = 0$, namely, once an sRNA-mRNA complex is formed, it goes to degradation rather than dissociate into its sRNA and mRNA components. Under this assumption, the level of the sRNA-mRNA complex, C, has no effect on the levels of other components in the MFL. Therefore, the set of four equations (1a)-(1d) can be integrated numerically or solved separately from Eq. (1e).

Under steady state conditions, the time derivatives on the left hand side of Eqs. (1) vanish, and the rate equations are reduced to a set of coupled algebraic equations. These

equations can be transformed into a single cubic equation of the form

$$\left(m-\frac{g_m}{d_m}\right)\left(m+\frac{d_s}{c_{ms}}\right)\left(m+\frac{u_g}{c_g}\frac{d_A}{g_A}\right)+\frac{u_g}{c_g}\frac{d_A}{g_A}\frac{g_s}{d_m}m=0 \tag{2}$$

For convenience we define the following dimensionless parameters: $M = g_m/d_m$, $D = d_s/c_{ms}$, $K = u_g d_A/(c_g g_A)$, and $S = g_s/d_m$. The parameter M represents the average number of mRNA molecules in the cell in the case that they are not regulated by sRNAs. The parameter D is the ratio between the probabilites that a single sRNA will degrade or bind to a single mRNA target. Therefore, D tends to decrease as the strength of the regulation by sRNAs increases. The parameter K is inversely proportional to the level of A proteins (when unregulated) and to their binding affinity to the b promoter. Therefore, K decreases as the transcriptional regulation of gene b becomes stronger. The parameter S represents the number of sRNA molecules which are transcribed during the average lifetime of an mRNA molecule. Using these parameters, we obtain a cubic equation for m of the form

$$m^3+a_2m^2+a_1m+a_0=0, \tag{3}$$

where $a_0 = -KDM$, $a_1 = K(D+S-M)-MD$ and $a_2 = D+K-M$. Depending on the values of the parameters, this equation may have either one or three real and positive solutions. In the first case, the system exhibits a single steady state. In the second case, it exhibits bistability, namely two stable steady states, while the third solution is unstable.

To analyze the existence and stability of the steady states of the MFL, it is useful to consider the bifurcation diagrams, presenting the steady state levels of A and s as a function of different parameters of the model. The stability of the solutions can be determined from the Jacobian of the set of rate equations and its eigenvalues.

In Figs. 2(a) and 2(c) we present the levels of the sRNA and the A protein under steady state conditions as a function of g_m, obtained analytically from the rate equations. For small values of g_m, a single steady state is observed, which is dominated by the sRNA. As g_m increases, a bifurcation takes place and a second steady state, dominated by A proteins, appears. A second bifurcation occurs at larger g_m value, beyond which only a single stable steady state remains, which is dominated by the A proteins. Similar results are presented in Figs. 2(b) and 2(d) as a function of g_s.

In order to extend and exemplify the robustness of the results presented above, in Appendix B we present the bifurcation diagrams of the MFL obtained for different binding

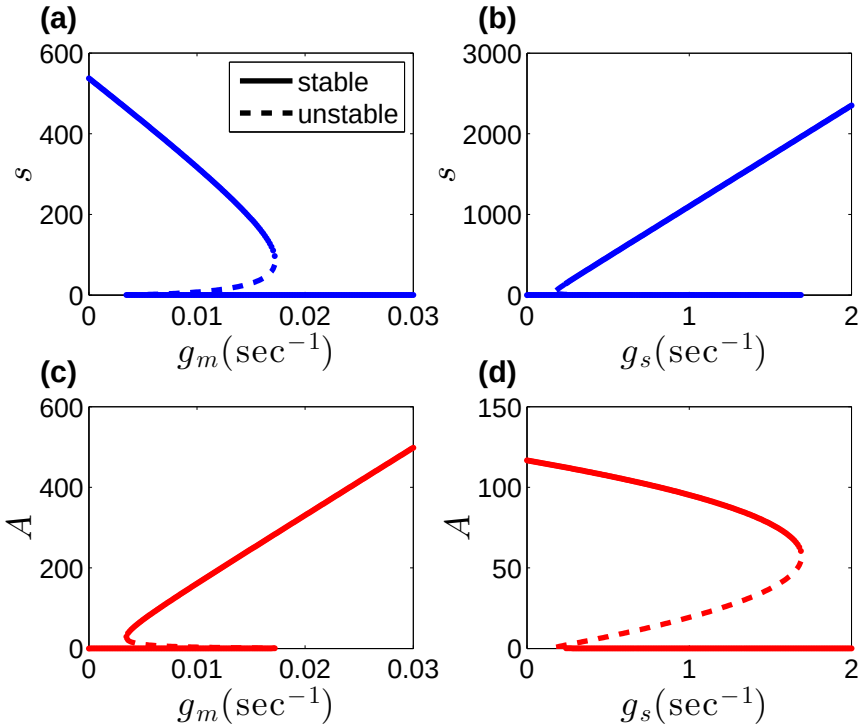

FIG. 2: (Color online) Bifurcation diagrams showing the levels of A and s as a function of the parameters g_m (a,c) and g_s (b,d). Solid lines represent stable solutions and dashed lines represent unstable solutions.

and unbinding kinetics of the TF to the sRNA promoter, a range of dissociation kinetics of the sRNA-mRNA complex, and different values of cooperativity of the TF to the sRNA promoter. In all cases, we observe a range of parameters in which bistability takes place.

III. STOCHASTIC ANALYSIS

In order to account for the effects of fluctuations in the MFL we analyze its dynamics using the master equation. Here the levels of the RNAs and protein take integer values, namely $m, A, s \in \mathbb{N}_0$, while the level of the bound repressor, $r \in \{0, 1\}$. The master equation accounts for the temporal variation of the probability distribution $P(m, A, r, s)$. It takes the form

$$
\begin{aligned}
\frac{dP(m,A,r,s)}{dt} &= g_m[P(m-1,A,r,s) - P(m,A,r,s)] \\
&+ g_s\delta_{r,0}[P(m,A,r,s-1) - P(m,A,r,s)] \\
&+ g_A m[P(m,A-1,r,s) - P(m,A,r,s)] \\
&+ c_{ms}[(m+1)(s+1)P(m+1,A,r,s+1) - msP(m,A,r,s)] \\
&+ c_g[(A+1)\delta_{r,1}P(m,A+1,0,s) - A\delta_{r,0}P(m,A,0,s)] \\
&+ u_g[\delta_{r,0}P(m,A-1,1,s) - \delta_{r,1}P(m,A,1,s)] \\
&+ d_m[(m+1)P(m+1,A,r,s) - mP(m,A,r,s)] \\
&+ d_A[(A+1)P(m,A+1,r,s) - AP(m,A,r,s)] \\
&+ d_s[(s+1)P(m,A,r,s+1) - sP(m,A,r,s)]. \qquad (4)
\end{aligned}
$$

where $\delta_{i,j} = 1$ for $i = j$ and 0 otherwise.

The first (second) term in this equation describes the transcription of mRNA (sRNA) molecules. The third term accounts for the translation of mRNAs into A proteins. The term involving c_{ms} describes the binding of sRNA and mRNA molecules, to form an sRNA-mRNA complex. The terms involving c_g and u_g, describe the binding and dissociation of A proteins to/from the promoter site of gene b, respectively. The last three terms correspond to the degradation of mRNAs, A proteins and sRNA molecules, respectively.

In order to examine the properties of the steady state solution of the master equation, it is useful to consider the marginal probability distribution

$$
P(A,s) = \sum_m \sum_r P(m,A,r,s), \qquad (5)
$$

In the formulation based on the master equation, the criterion for bistability is that the steady state solution $P(A,s)$ exhibits two distinct peaks, separated by a gap in which the probabilities are low. The locations of these peaks on the (A,s) plane correspond to the two bistable solutions of the rate equations.

In order to obtain the switching times between the two bistable states and estimate the probability distributions of the different possible discrete states of the system, we perform Monte Carlo (MC) simulations using the Gillespie algorithm [41]. This is a kinetic MC approach, namely, an algorithm that generates 'paths' of the stochastic process. At each

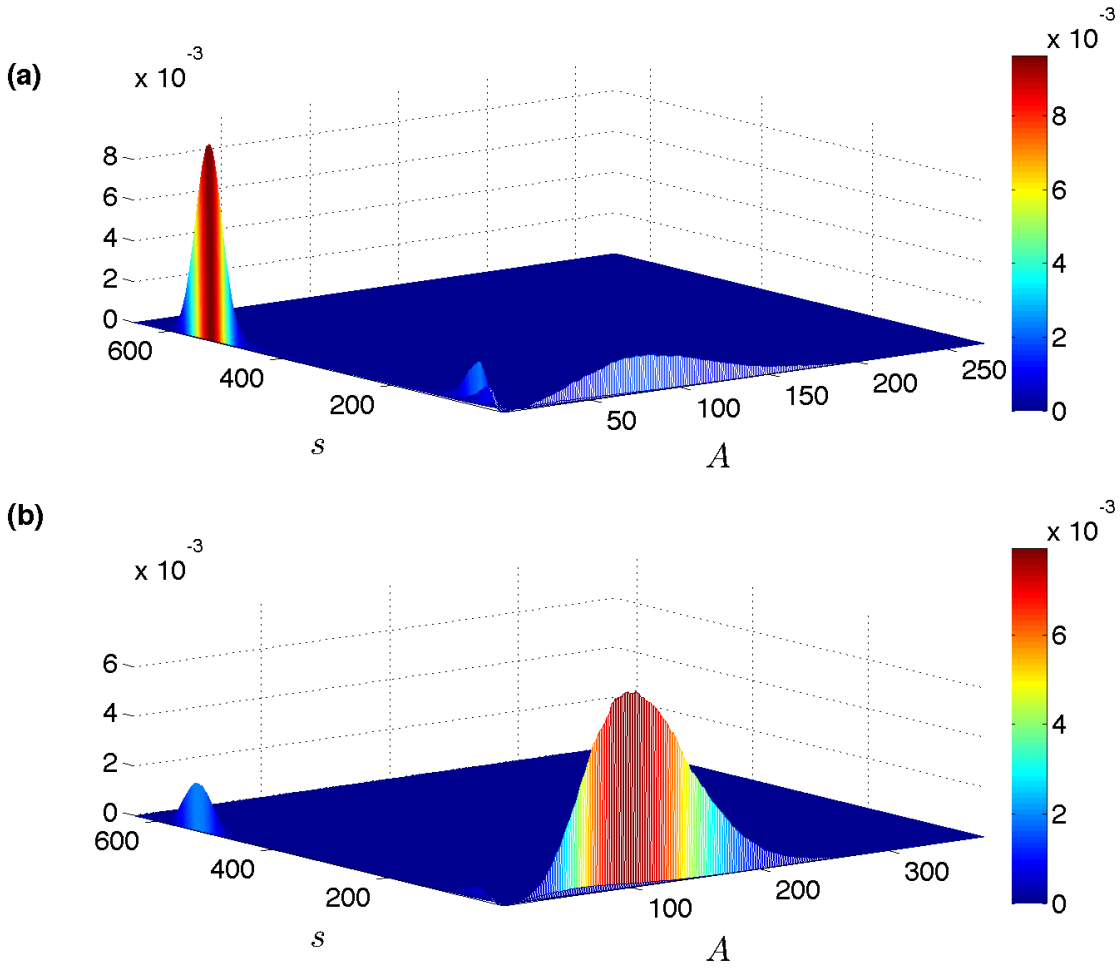

FIG. 3: (Color online) The probability distribution $P(A, s)$ for the MFL: (a) in the state dominated by the sRNA regulator (obtained for $g_m = 0.0058$ sec^{-1}); and (b) for the state dominated by the transcriptional repressor (obtained for $g_m = 0.0071$ sec^{-1}).

time step the next move is drawn from all possible processes that may take place at that point, where each step is endowed with a suitable weight. After each move, the elapsed time is properly advanced, the list of available processes is updated and their new rates are evaluated.

In Fig. 3 we present the probability distribution $P(A, s)$, generated by performing MC simulations (10^7 sec each), and quantifying the relative fraction of time in which the system is found in each discrete $P(A, s)$ state, averaged over initiations of the system at both the sRNA and TF dominated states. The probability distribution is presented for conditions under which the system is dominated by the sRNA regulator [Fig. 3(a)] and for conditions

under which it is dominated by the transcriptional repressor [Fig. 3(b)]. In both cases the distribution exhibits two peaks representing the two bistable states. In the former case the peak dominated by sRNAs is large and the peak dominated by transcriptional repressors is small, while in the latter case the situation is reversed. The peak dominated by sRNAs is sharp and narrow while the peak dominated by the transcriptional repressors is broad. The volume of each peak represents the cumulative probability of microscopic states associated with the corresponding state of the system. It also represents the fraction of the time in which the system is expected to reside in that state.

We denote the mean lifetimes of the bistable states dominated by the sRNA and by the transcriptional repressor by τ_s and τ_A, respectively. To obtain the values of τ_s (τ_A) we initialize the system in the state dominated by the sRNA (transcriptional repressor) and evaluate the average time elapsed until a transition to the A (s) dominated state has occurred. The transition between states is defined as the point in which the level of the previous minority species exceeds that of the dominant species.

In Fig. 4 we present a typical result of an MC simulation of the MFL. The system is clearly bistable, with spontanous fluctuation-driven switching transitions. In the sRNA dominated state there are failed switching attempts, corresponding to the third, unstable steady state, in which the sRNA level is reduced, but is then recovered. In the A dominated state, both the mRNA and protein levels exhibit large fluctuations, accompanied by fast binding/unbinding of A proteins to/from the b promoter.

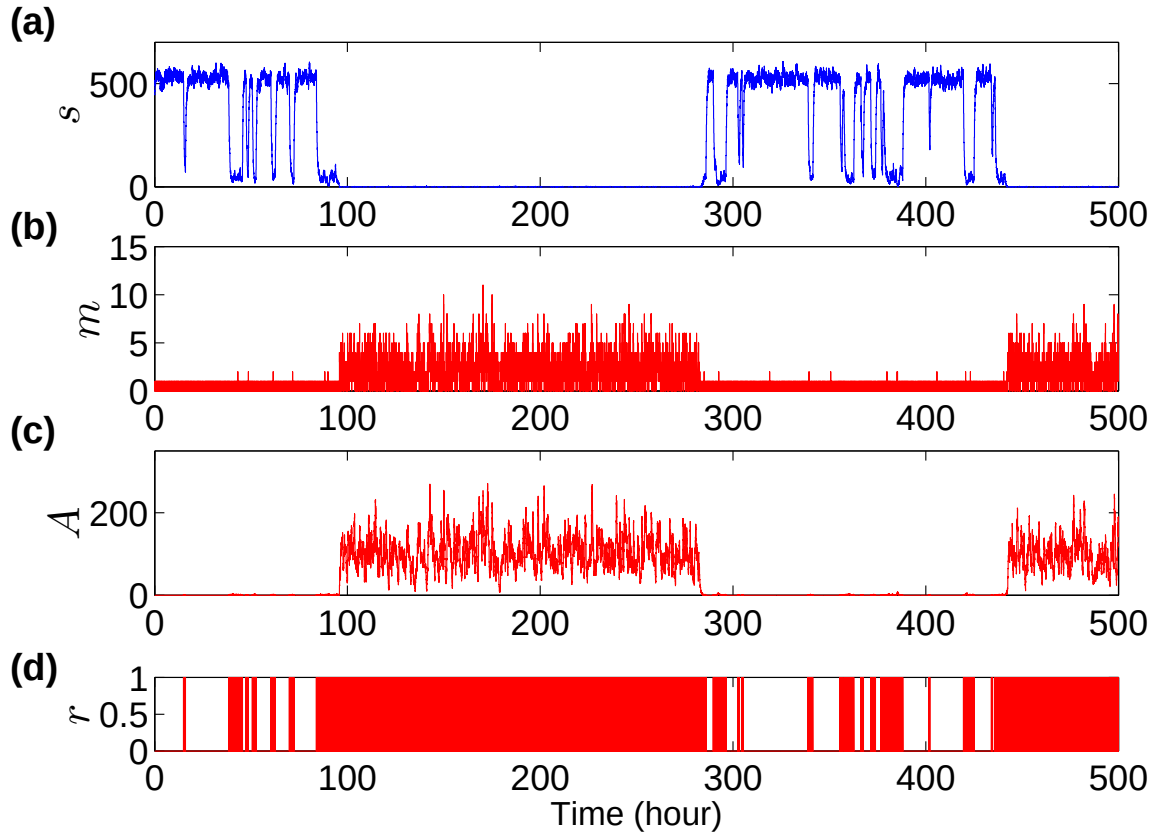

FIG. 4: (Color online) The levels of the sRNAs (a), mRNAs (b), free A repressors (c) and bound repressors (d) vs. time in the MFL, obtained from Monte Carlo simulations. Failed attempts to transition from the s to the A dominated state are observed, following periods in which the s promoter is occupied by the transcriptional repressor.

To examine the dependence of the lifetimes of the two bistable states on parameters, we present in Fig. 5 the lifetime of the sRNA dominated state, τ_s, as a function of the transcription rates of the mRNA and sRNA. As the transcription rate g_m, is increased, the switching rate from the state dominated by the sRNA to the state dominated by the transcriptional repressor increases and the lifetime, τ_s, of the sRNA dominated state decreases [Fig. 5(a)]. On the other hand, when the transcription rate of the sRNA, g_s, is increased, the lifetime of the sRNA dominated state, τ_s, increases [Fig. 5(b)].

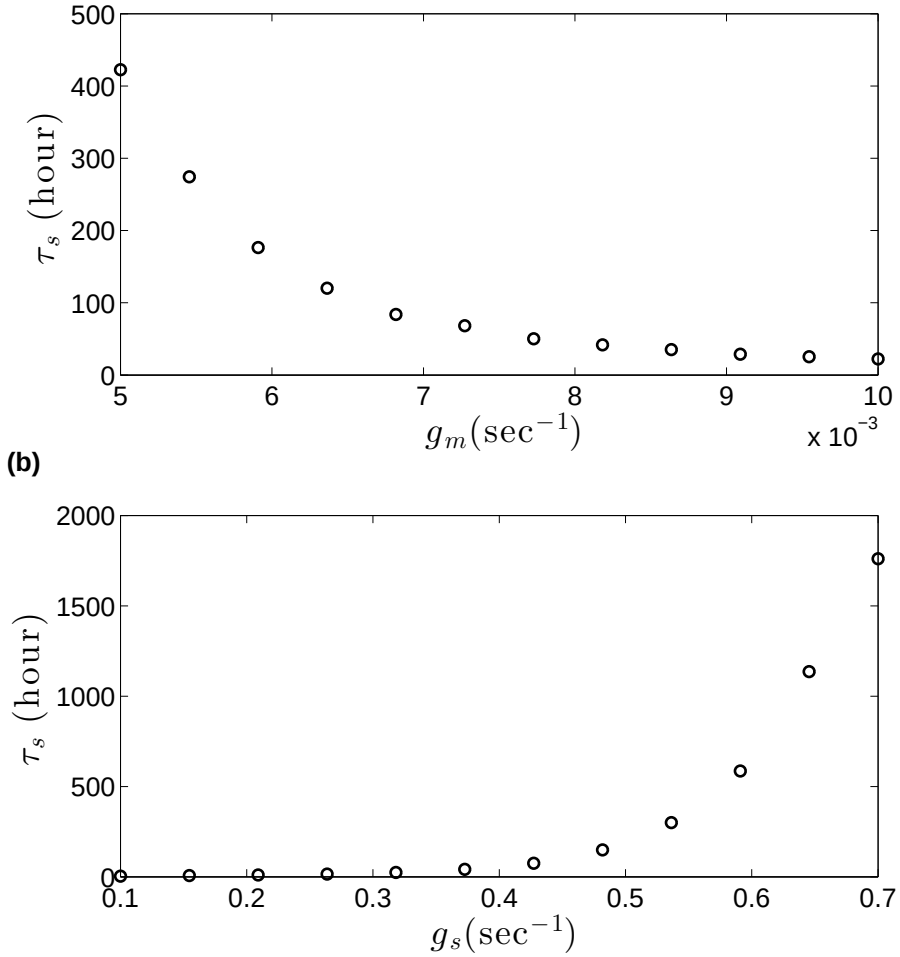

FIG. 5: The average lifetime of the sRNA dominated state, τ_s, as a function of the parameters g_m (a) and g_s (b), obtained from MC simulations. The lifetime τ_s monotonically decreases with g_m and monotonically increases with g_s. Each data point was averaged over 1000 MC runs.

Further insight into the balance between the two bistable states can be obtained by evaluating the fraction of the time in which the system resides in each state. The fraction of time in which the sRNA is dominant is given by

$$P_s = \frac{\tau_s}{\tau_A + \tau_s}, \tag{6}$$

while the fraction of time the transcriptional repressor is dominant is $P_A = 1 - P_s$.

In Fig. 6(a) we present the bifurcation diagram for the sRNA level vs. g_m, obtained from the rate equations, showing the range of g_m values in which bistability takes place. In Fig. 6(b) we present the fraction of time, P_s, in which the system resides in the sRNA dominated state vs. g_m, obtained from MC simulations. P_s follows a decreasing sigmoid function vs. g_m. In the limit in which g_m is small the system spends most of its time in the sRNA dominated state, while in the large g_m limit it spends most of the time in the state dominated by the transcriptional repressor. It is found that in both limits, the MFL is biased towards one of the steady states.

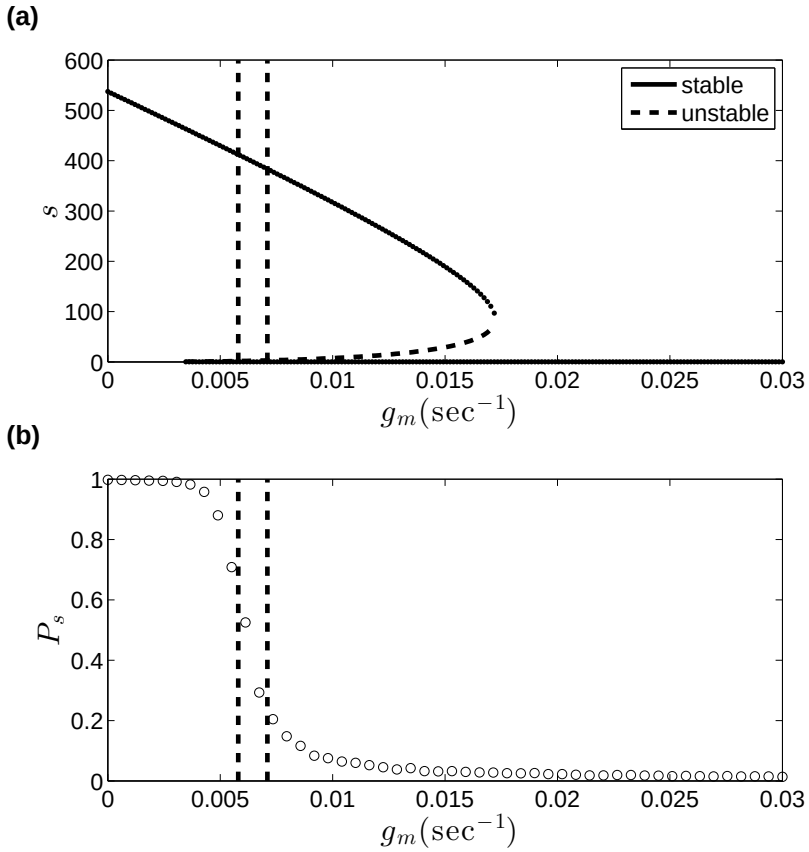

FIG. 6: (a) The sRNA level, s, as a function of the transcription rate g_m, obtained from the rate equations. (b) The fraction of time, P_s, that the system resides in the sRNA dominated state vs. g_m, obtained from MC simulations. The dependence of P_s on g_m is of the form of a decreasing sigmoid function. Two vertical lines mark the g_m values, as shown in Fig. 3, for the state dominated by the sRNA regulator (obtained for $g_m = 0.0058$ sec^{-1}), and for the state dominated by the transcriptional repressor (obtained for $g_m = 0.0071$ sec^{-1}).

IV. SUMMARY AND DISCUSSION

We have performed deterministic and stochastic analyses of the double-negative mixed feedback loop involving transcriptional regulation and post-transcriptional regulation via sRNA-mRNA interaction. Using deterministic methods, we identified the range of parameters in which these systems exhibit bistability. We have shown that within this range, the relative lifetimes of the two stable states (P_s and P_A) follow complementary sigmoid functions as parameters such as the transcription rates are varied. Different P_s values may be beneficial for MFLs, or other bistable systems, under different biological contexts, yielding, at the population level, a bimodal distribution. Indeed, the relative lifetimes of biological bistable systems were extensively studied and were shown (both theoretically and experimentally) to exhibit a wide range of values [20, 21, 42–46].

An important example of a double-negative MFL appears in *E. coli*, consisting of the genes *fur* (encoding a transcriptional repressor) and *ryhB* (encoding an sRNA). In presence of iron, the Fur repressor is active, repressing the transcription of the RyhB sRNA, as well as other genes involved in iron metabolism [25–27]. Thus, *fur* plays the role of gene a in Fig. 1. When iron supply is limited, Fur becomes inactive and RyhB is transcribed. Fur synthesis is translationally coupled to that of an upstream open reading frame, whose translation is downregulated by RyhB [27]. Therefore, *ryhB* plays the role of gene b in Fig. 1. When the iron level increases and the stress condition is removed, the level of Fur is restored and overrides the RyhB sRNA [26]. Another relevant example of a double-negative MFL in *E. coli* consists of the global transcriptional regulator Lrp and the sRNA MicF [28]. Lrp activates genes that need to be expressed under nutrient-poor conditions while repressing genes that need to be expressed under nutrient-rich conditions. Accordingly, it was shown that Lrp is highly expressed under nutrient-poor conditions, while MicF is highly expressed under nutrient rich conditions. The results presented in this paper shed further light on the sensitivity of the dynamics of such MFLs to changes in effective parameters by external conditions, determining which of the two regulators dominates under given conditions, and to what extent.

V. ACKNOWLEDGEMENTS

This work was supported by grants from Israel Science Foundation and the Israel Ministry of Science and Technology granted to HM. MN is grateful to the Azrieli Foundation for the award of an Azrieli Fellowship.

Appendix A: Rate coefficients

The equations that describe the MFL include a large number of rate coefficients for the rates of the transcription, translation, binding, unbinding and degradation processes. To obtain results and predictions that are biologically meaningful, one should use rate coefficients that are in the biologically relevant range. While the analysis performed in this paper is quantitative, the conclusions are of a qualitative nature and describe the generic behavior of the MFL. Below we discuss in more detail the considerations we have made in order to identify the biologically relevant range of each parameter.

1. Transcription and degradation rates of mRNAs

Previous analyses have revealed that the rate limiting step in the transcription is usually the delay between the binding of RNA polymerase to the promoter site and the beginning of the elongation process [47]. Measurements have shown that this time lag exhibits great variation between different genes and under different conditions, and takes values between 20 seconds and 10 minutes. The delay time can be represented by the transcription initiation rate, taking values in the range $0.001 \leq g_m \leq 0.05$ molecules per second. Recent measurements of mRNAs in single cells showed that for the gene that was studied, an mRNA molecule is produced every 7 minutes, which amounts to a transcription rate of $g_m = 0.0024$ (sec^{-1}) [48]. The half life of mRNA is typically in the range between 30 and 300 (sec). This yields mRNA degradation rates in the range $0.003 \leq d_m \leq 0.03$ (sec^{-1}).

2. Transcription and degradation rates of sRNAs

An example of a small RNA in *E. coli*, on which extensive experimental measurements were performed is OxyS. This sRNA appears in high copy numbers [49]. In the absence of

target mRNAs, it was found to have a half-life of 12-15 minutes, which is longer than most mRNAs (with typical half-life of 2-4 min). In order to allow for variations between different sRNAs, we choose a broader range of half life values, translating to sRNA degradation rates in the range $0.0002 \leq d_s \leq 0.002$ ($\sec^{-1}$).

Values reported for generation rates of various sRNAs were in the range $0.02 \leq g_s \leq 7.5$ ($\sec^{-1}$). The lower limit was reported in [4]. The upper Limit was obtained by assuming that the steady state level of oxyS was due to synthesis and degradation processes, $g_s = s \times d_s = 4500 \times (0.0005 - 0.00167\ \sec^{-1})$ [49] $= 2.5 - 7.5\ \sec^{-1}$.

3. Protein synthesis and degradation rates

Measurements of protein synthesis rates are reported in Ref. [50]. It was shown that a protein can be translated from each mRNA molecule every 3-4 seconds. To cover a broad range of biologically relevant translation rates, we take the range of 2-20 seconds. This corresponds to translation rate coefficients in the range $0.05 \leq g_A \leq 0.5$ ($\sec^{-1}$).

Transcription factors are usually short lived, with half life of a few minutes. Thus, we consider degradation rates in the range $0.001 \leq d_A \leq 0.05$ ($\sec^{-1}$).

4. Binding rates of sRNAs to their mRNA targets

Measurements of the binding of the sRNA OxyS to its mRNA target *fhlA*, performed in vitro, are reported in Ref. [49]. In these experiments 2nM of the OxyS sRNA were mixed with different concentrations of the *fhlA* mRNA. After 5 minutes the concentration of free OxyS was measured. It was found that when the concentration of the *fhlA* mRNA was 25nM, half of the OxyS molecules were bound after 5 minutes. This was done in vitro, where the synthesis of new sRNA and mRNA molecules as well as their degradation were suppressed. Denoting the level of OxyS by s and of the *fhla* mRNA by m, the dynamics can be described by

$$\begin{aligned} \frac{ds}{dt} &= -c_{ms} m \cdot s \\ \frac{dm}{dt} &= -c_{ms} m \cdot s. \end{aligned} \tag{A1}$$

This means that under these conditions the difference between the levels of m and s remains

constant. Assuming that the initial levels at time $t = 0$ satisfy $m_0 > s_0$, we can solve this equation and obtain

$$\begin{aligned} s(t) &= \frac{(m_0 - s_0)s_0}{m_0 \exp[c_{ms}(m_0 - s_0)t] - s_0} \\ m(t) &= \frac{(m_0 - s_0)m_0}{m_0 - s_0 \exp[-c_{ms}(m_0 - s_0)t]}. \end{aligned} \tag{A2}$$

Setting the initial conditions and fitting the binding rate coefficient c_{ms} such that after 5 minutes the sRNA concentration s goes down to a half of the initial concentration s_0, we obtain that $c_{ms} = 9.45 \times 10^{-5} (\text{nM} \cdot \text{sec})^{-1}$. Taking the *E. coli* cell volume as 10^{-15} liters, we obtain 1nM=0.6 molecules per cell, giving $c_{ms} = 0.0002$ (sec^{-1}). Since this experiment was carried out without Hfq, which is a catalyst of the reaction, it is reasonable to take a range of c_{ms} values which express faster binding. This would most likely also account for variations in the binding rates of other sRNA molecules to other mRNAs. We therefore take the range $0.001 \leq c_{ms} \leq 0.02$ (sec^{-1}).

5. Transcription factor binding/unbinding rates

The binding and unbinding rates of two transcription factors in two *E. coli* strains to/from their specific promoter sites on the DNA were measured in Ref. [51]. Using surface plasmon resonance, which can monitor the time dependent changes in concentrations, they found binding rates of $0.09 - 0.14$ (sec^{-1}). This means that a transcription factor would bind to the DNA within 7-11 seconds. Measuring the ratio between bound and free DNA yields the ratio between the binding and dissociation rates. The values that were obtained for the dissociation rate are in the range of $0.001 - 0.002$ (sec^{-1}). This in turn means that a transcription factor stays bound to the promoter site for 1000 to 2000 seconds. To make the range more dynamic and account for weaker transcriptional repression we choose the ranges $0.05 \leq c_g \leq 0.25$ (sec^{-1}), and $0.001 \leq u_g \leq 0.01$ (sec^{-1}).

Appendix B: Extended stability analysis

Here we investigate how the MFL bifurcation diagram is affected by a broad family of parameter variations and modifications of the network. In Fig. 2 we showed the bifurcation diagrams for the parameters g_m and g_s, representing the transcription rates of the TF and

sRNA, respectively. Here we further present the bifurcation diagrams for the binding and unbinding rates of the TF to the sRNA promoter, denoted by c_g and u_g, respectively, and the dissociation rate of the sRNA-mRNA complex, denoted by u_c. In addition, we examine the effect of cooperativity of the binding of the TF, A, to the sRNA promoter which is characterised by the Hill coefficient α. The rate equations describing the MFL with cooperative binding take the form

$$\frac{dm}{dt} = g_m - d_m m - c_{ms} m \cdot s + u_c C \tag{B1a}$$

$$\frac{ds}{dt} = g_s(1-r) - d_s s - c_{ms} m \cdot s + u_c C \tag{B1b}$$

$$\frac{dA}{dt} = g_A m - d_A A - \alpha c_g A^\alpha (1-r) + \alpha u_g r \tag{B1c}$$

$$\frac{dr}{dt} = c_g A^\alpha (1-r) - u_g r \tag{B1d}$$

$$\frac{dC}{dt} = c_{ms} m \cdot s - d_c C - u_c C \ . \tag{B1e}$$

For the results presented below, we take the following default parameter values: g_m=0.007, g_s=0.43, g_A=0.05, d_m=0.003, d_s=0.0008, d_A=0.001, c_{ms}=0.02, c_g=0.08, u_g=0.01, d_c=0.003, α=1. All the parameters are in units of $\sec^{-1}$, except for α which is dimensionless. In Figs. 7(a,b) and 7(d,e) we present the levels of the sRNA and the A protein under steady state conditions as a function of c_g and u_g, respectively, obtained analytically from the rate equations. The ranges of c_g and u_g agree with those presented in Appendix A. As expected, the effect of c_g (binding of the TF to the sRNA promoter) opposes that of u_g (unbinding); as c_g increases or u_g decreases, the TF strengthens its repressive role over the sRNA. More specifically, for small values of c_g, a single steady state, dominated by the sRNA, is observed. As c_g increases, a bifurcation takes place and a second steady state, dominated by A proteins, appears. A second bifurcation occurs at larger c_g value, beyond which only a single stable steady state remains, which is dominated by the A proteins. For small values of u_g, a single steady state, dominated by the TF, is observed, As u_g increases, a bifurcation takes place and a second steady state, dominated by the sRNA, appears. In Figs. 7(c) and 7(f) we present the levels of the sRNA and the A protein as a function of u_c. Here, increasing u_c 'weakens' the sRNA state, yielding, following a bifurcation, a single steady state, dominated by A.

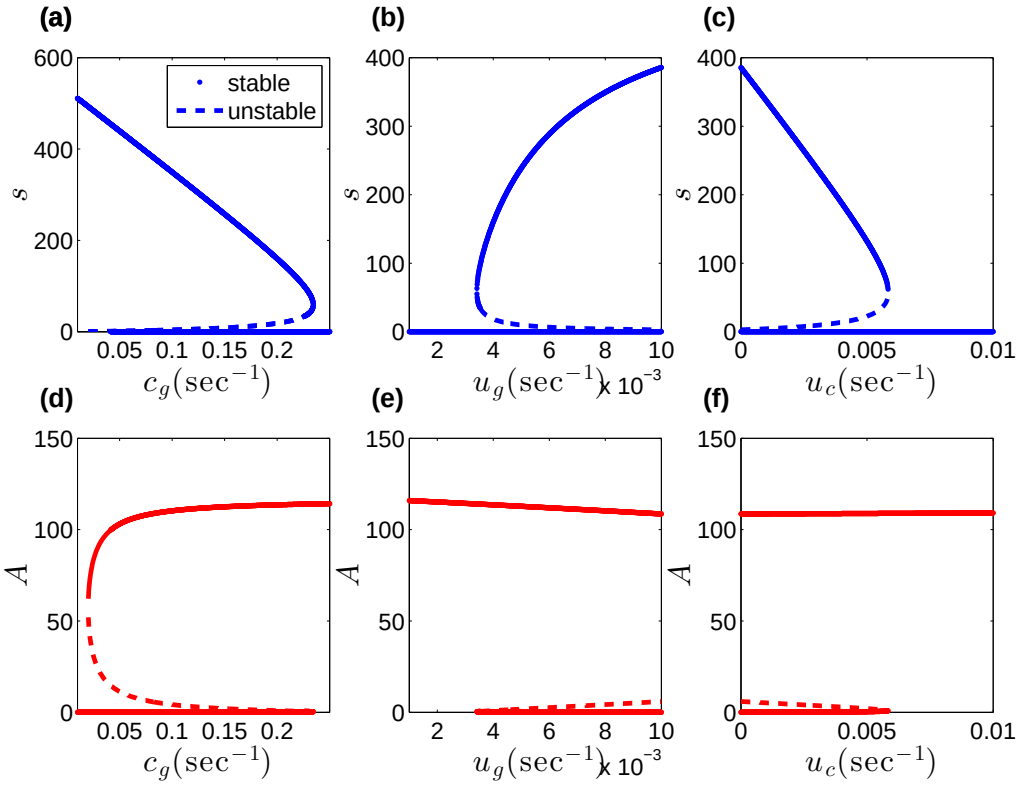

FIG. 7: (Color online) Bifurcation diagrams showing the levels of A and s as a function of the parameters c_g (a,d), u_g (b,e), and u_c (c,f). Solid lines represent stable solutions and dashed lines represent unstable solutions.

Next, we consider the effect of the cooperativity, as expressed by the Hill coefficient α in Eq. B1, of the binding of the TF protein to the sRNA promoter on the stability. In Fig. 8 we present the bifurcation diagram showing the level of s as a function of g_m, for different values of α ($\alpha = 1, 2, 5$). The range of g_m agrees with that presented in Appendix A. As expected, as cooperativity increases, the repression by A weakens and the s state strengthens. This is expressed as a higher-level steady state and delayed bifurcation (in terms of g_m) for higher α, as can be seen in Fig. 8. Note that for $\alpha = 1$, c_g is simply the binding rate of the transcriptional repressor to the sRNA promoter. For $\alpha > 1$, it represents the overall rate of a more complicated process, which includes the assembly of a repressor complex of α repressors, and its binding to the promoter site.

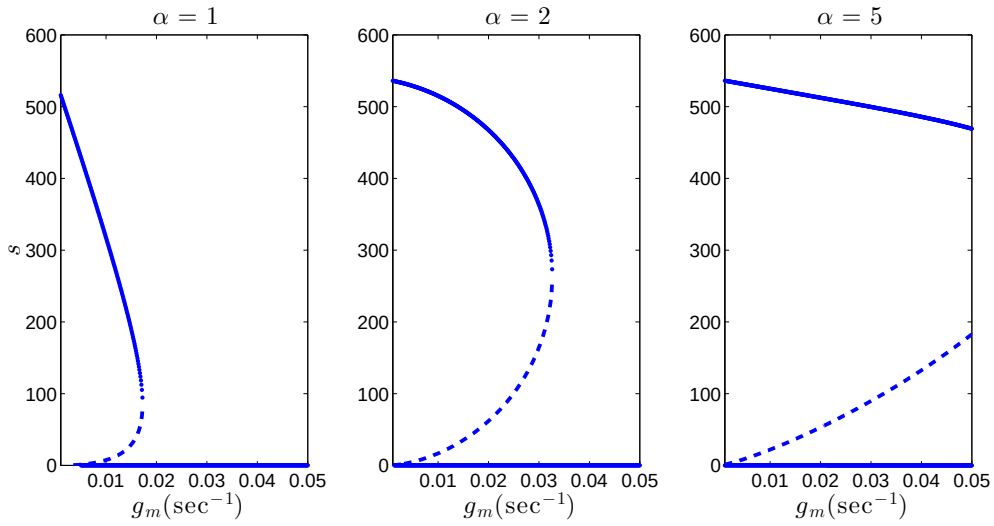

FIG. 8: Bifurcation diagrams showing the level of s as a function of the parameter g_m, for different values of α. Solid lines represent stable solutions and dashed lines represent unstable solutions.

---

[1] G. Storz, S. Altuvia, and K. M. Wasserman, Annu. Rev. Biochem. **74**, 199 (2005).

[2] S. Gottesman, Trends Genet. **21**, 399 (2005).

[3] R. Hershberg, S. Altuvia, and H. Margalit, Nucleic Acids Res. **31**, 1813 (2003).

[4] T. K. E. Levine, Z. Zhang and T. Hwa, PLoS Biol **5**, e229 (2007).

[5] E. G. S. Altuvia and H. Wagner, Proc. Natl. Acad. Sci. US **97**, 9824 (2000).

[6] S. Gottesman and G. Storz, Cold Spring Harb Perspect Biol. **3**, 1 (2011).

[7] C. Baker, T. Jia, and R.V. Kulkarni, Phys. Rev. E **85**, 061915 (2012).

[8] Y. Shimoni, G. Friedlander, G. Hetzroni, G. Niv, S. Altuvia, O. Biham, and H. Margalit, Mol. Sys. Biol. **3:138**, 5 (2007).

[9] P. Mehta, S. Goyal and N.S. Wingreen, Mol. Sys. Biol. **4**, 221 (2008).

[10] R. Milo, S. Shen-Orr, S. Itzkovitz, N. Kashtan, D. Chklovskii, and U. Alon, Science **298**, 824 (2002).

[11] S. S. Shen-Orr, R. Milo, S. Mangan, and U. Alon, Nature Genetics **31**, 64 (2002).

[12] E. Yeger-Lotem and H. Margalit, Nucleic Acids Res. **31**, 6053 (2003).

[13] E. Yeger-Lotem, S. Sattath, N. Kashtan, S. Itzkovitz, R. Milo, R. Y. Pinter, U. Alon, and H.

Margalit, Proc. Natl. Acad. Sci. US **101**, 5934 (2004).

[14] L. V. Zhang, O. D. King, S. L. Wong, D. S. Goldberg, A. H. Tong, G. Lesage, B. Andrews, H. Bussey, C. Boone, and F. P. Roth, J. biol. **4**, 6 (2005).

[15] P. Mandin and M. Guillier, Current Opinion Microbiol. **16**, 125 (2013).

[16] M. Ptashne, *A Genetic Switch: Phage λ and Higher Organisms, 2nd edition.* (Cell Press and Blackwell Scientific Publications, Cambridge, MA, 1992).

[17] T. S. Gardner, C. R. Cantor, and J. J. Collins, Nature **403**, 339 (2000).

[18] J.L. Cherry and F.R. Adler, J. Theor. Biol. **203**, 117 (2000).

[19] T. B. Kepler and T. C. Elston, Biophys. J. **81**, 3116 (2001).

[20] P. B. Warren and P. R. ten Wolde, Phys. Rev. Lett. **92**, 128101 (2004).

[21] P. B. Warren and P. R. ten Wolde, J. Phys. Chem. B **109**, 6812 (2005).

[22] A. M. Walczak, M. Sasai, and P. Wolynes, Biophys. J. **88**, 828 (2005).

[23] A. Lipshtat, A. Loinger, N. Q. Balaban, and O. Biham, Phys. Rev. Lett. **96**, 188101 (2006).

[24] A. Loinger, A. Lipshtat, N. Q. Balaban, and O. Biham, Phys. Rev. E **75**, 021904 (2007).

[25] E. Massé, C. K. Vanderpool, and S. Gottesman, J. Bacteriol. **187**, 6962 (2005).

[26] E. Massé, H. Salvail, G. Desnoyers, and M. Arguin, Current Opinion Microbiol. **10**, 140 (2007).

[27] B. Vecerek, I. Moll, and U. Blasi, EMBO J. **26**, 965 (2007).

[28] E. Holmqvist, C. Unoson, J. Reimegard and E.G.H. Wagner, Mol. Microbiol. **84**, 414 (2012).

[29] F. Fazi, A. Rosa, A. Fatica, V. Gelmetti, M. L. D. Marchis, C. Nervi, and I. Bozzoni, Cell **123**, 819 (2005).

[30] S. Fujita, T. Ito, T. Mizutani, S. Minoguchi, N. Yamamichi, K. Sakurai, and H. Iba, J. Mol. Biol. **378**, 492 (2008).

[31] L. Fontana, E. Pelosi, P. Greco, S. Racanicchi, U. Testa, F. Liuzzi, C. M. Croce, E. Brunetti, F. Grignani, and C. Peschle, Nat. Cell Biol. **9**, 775 (2007).

[32] J. Varhese and S. M. Cohen, Genes & Dev. **21**, 2277 (2008).

[33] K. C. Tu, C. M. Waters, S. L. Svenningsen, and B. L. Bassler, Mol. Microbiol. **70**, 896 (2008).

[34] R. J. Johnston, S. Chang, J. F. Etchberger, C. O. Ortiz, and O. Hobert, Proc. Natl. Acad. Sci. US **102**, 12449 (2005).

[35] B. Novak and J. J. Tyson, Nat Rev Mol Cell Biol **9**, 981 (2008).

[36] P. François and V. Hakim, Phys. Rev. E **72**, 031908 (2005).

[37] D. Liu, X. Chang, Z. Liu, L. Chen and R. Wang, Plos One **6**, e17029 (2011).

[38] P. Zhou, S. Cai, Z. Liu and R. Wang, Phys. Rev. E **85**, 041916 (2012).

[39] S. Wang and S. Raghavachari, Phys. Biol. **8**, 055002 (2011).

[40] J. Lloyd-Price and A. S. Ribeiro, Phys. Rev. E **88**, 032714 (2013).

[41] D. T. Gillespie, J. Phys. Chem. **81**, 2340 (1977).

[42] M. Acar, A. Becskei, and A. van Oudenaarden, Nature **435**, 228 (2005).

[43] N. Mirouze, Y. Desai, A. Raj, and D. Dubnau, PLoS genetics **8**, e1002586 (2012).

[44] M. Santilln, Biophys. J. **94**, 2065 (2008).

[45] H. Maamar, A. Raj, and D. Dubnau, Science **317**, 526 (2007).

[46] F. J. Isaacs, J. Hasty, C. R. Cantor, and J. J. Collins, Proc. Natl. Acad. Sci. US **100**, 7714 (2003).

[47] W. R. McClure, Proc. Natl. Acad. Sci. US **77**, 5634 (1980).

[48] I. Golding, J. Paulsson, S. M. Zawilski, and E. C. Cox, Cell **123**, 1025 (2005).

[49] S. Altuvia, D. WeinsteinFischer, A. Zhang, L. Postow, and G. Storz, Cell **90**, 43 (1997).

[50] D. Kennell and H. Riezmak, J. Mol. Biol. **114**, 1 (1977).

[51] P. Henriksson-Peltola, W. Sehln, and E. Haggrd-Ljungquist, Nucleic Acids Res. **35**, 3181 (2007).